

UnderOak Observer

Issue 4 · April - June 2012

**A Fresh Look at the Algol-like
Eclipsing Binary AO Serpentis**

**Lightcurve Analysis of
201 Penelope and 360 Carlova**

CCD Monitoring of a Supernova: SN 2012aw

Lightcurve Analysis of Two Main Belt Minor Planets



Abstract

Fourier analyses of CCD derived lightcurves produced synodic period solutions for 201 Penelope (3.7491 ± 0.0012 h) and 360 Carlova (6.1894 ± 0.0003 h).

Introduction

The instrument used at UnderOak Observatory (UO) is a 0.2 m catadioptric OTA (f/7) equipped with an SBIG ST402ME thermoelectrically-cooled CCD. The optical assembly produces a field-of-view approximating 11×17 arcmin (1.33 arcsec/pixel). Photometric acquisition conditions and image reduction typically used at UO have been published in greater detail (Alton 2010). Unfiltered 60-s (201 Penelope) or I_c filtered 90-s (360 Carlova) exposures were continually captured during each session lasting from 3.5 to 6 h. Data were light time corrected and reduced to instrumental magnitudes with MPO Canopus (Warner 2010). At least 2 non-varying comparison stars were used to generate lightcurves by differential aperture photometry. Fourier analysis (Harris 1989) yielded a period solution from each folded dataset and then independently verified using Peranso (Vannmunster 2006) as previously described (Alton 2011). Relevant aspect parameters for each of these main belt asteroids taken at the mid-point from each observing session are tabulated below. Phased data are available upon request (mail@underoakobservatory.com).

Results and Discussion

201 Penelope Discovered in 1879 by Johan Palisa this M-type asteroid ($D=68$ km) has been studied by numerous investigators mostly over the past three decades. Photometric studies which initially established the color index and/or determined its synodic period include Lagerkvist et al 1981, Surdej et al 1983, and Pfleiderer et al 1987. A

spectrophotometric ($0.338\text{--}0.762$ μm) analysis of surface material (Busarev 1998) revealed the presence of hydrated silicates. Physical modeling of this asteroid (Torppa et al 2003) suggests a quite regular triaxial ellipsoid shape ($a/b = 1.5$ and $b/c = 1.1$). At UO, a total of 555 images were taken over 2 nights (2011 Dec 10 and 2011 Dec 11). Lightcurve analysis (Figure 1) produced the best folded fit at a slightly longer period (3.7491 h) than the value (3.7474 h) presently posted at the JPL Solar System Dynamics website (<http://ssd.jpl.nasa.gov/sbdb.cgi>). The peak-to-peak amplitude (0.16 mag) observed during this most recent apparition was within the range ($0.15\text{--}0.73$ mag) reported for this object by Foglia et al (2000).

360 Carlova This sizeable C-type asteroid ($D=116$ km) was discovered by Auguste Charlois in 1893. Harris and Young (1983) published the earliest lightcurve followed by similar investigations from DiMartino et al (1987), Michalowski et al (2000), Wang (2002), and Wang and Zhang (2006). More recently Durech et al (2009) published a spin-state solution for 360 Carlova using a combination of sparse and dense photometric data. During the CCD photometric study at UO, 750 images were acquired on four nights between 2012 Feb 01 and 2012 Feb 18. The synodic period solution (6.1894 h) estimated by MPO Canopus was very similar to the composite value (6.1896 h) recently reported by Durech et al (2009). This lightcurve exhibited a peak-to-peak amplitude (0.38 mag) which was within the range ($0.30\text{--}0.49$ mag) estimated from all the lightcurves referenced herein (Figure 2).

Acknowledgement

Many thanks to the SAO/NASA Astrophysics Data System and the Asteroid Lightcurve Database (LCDB),

Object	Range Over Observation Period			
	UT Date	Phase Angle	L_{PAB}	B_{PAB}
201 Penelope	2011 Dec 10 – 2011 Dec 11	13.9 - 14.2	48.8 - 48.9	(-7.2) – (-7.2)
360 Carlova	2012 Feb 01 – 2012 Feb 18	9.2 – 15.0	111.2 – 112.3	(-4.4) – (-3.2)

both of which proved indispensable for locating relevant literature references.

References

- Alton, K.B. (2010), "A Unified Roche-Model Light Curve Solution for the W UMa Binary AC Bootis", JAAVSO 38.
- Alton, K.B. (2011), "CCD Lightcurves for 4 Main Belt Asteroids", Minor Planet Bulletin 38, 8-9.
- Busarev, V.V. (1998), "Spectral Features of M-Asteroids: 75 Eurydike and 201 Penelope", Icarus 131, 32-40.
- DiMartino, M., Zappala, V., DeCampos, J.A., Debehogne, H. and Lagerkvist, C.-I. (1987), "Rotational Properties and Lightcurves of the Minor Planets 94, 107, 197, 201, 360, 451, 511 and 702", Astron. Astrophys. Suppl. Ser. 67, 95-101.
- Durech, J., Kaasalainen, M., Warner, B.D., Fauerbach, M., Marks, S.A., Fauvaud, S., Fauvaud, M., Vugnon, J.-M., Pilcher, F., Bernasconi, L. and Behrend, R. (2009), "Asteroid Models From Combined Sparse and Dense Photometric Data", Astron. Astrophys. 493, 291-297.
- Foglia, S., Marchis, F., Morecchio, J.G., Elchiver, M.A.A. and Wicha, F.J.L., "Photometry of 201 Penelope from Chile and Italy", Minor Planet Bulletin 27, 52-53.
- Lagerkvist, C.-I., Rickman, H., Scaltriti, F. and Zappala, V. (1981), "Physical Studies of Asteroids: VI. Asteroid 201 Penelope, a Fast Rotator", Astron. Astrophys. 104, 148-149.
- Harris, A.W. and Young, J.W. (1983), "Asteroid rotation. IV", Icarus 54, 59-109.
- Harris, A.W., Young, J.W., Bowell, E., Martin, L. J., Millis, R. L., Poutanen, M., Scaltriti, F., Zappala, V., Schober, H. J., Debehogne, H. and Zeigler, K. (1989), "Photoelectric Observations of Asteroids 3, 24, 60, 261, and 863." Icarus 77, 171-186.
- Michalowski, T., Pych, W., Berthier, J., Kryszczyńska, A., Kwiatkowski, T., Boussuge, J., Fauvaud, S., Denchev, P. and Baranowski, R. (2000), "CCD Photometry, Spin and Shape Models of Five Asteroids: 225, 360, 416, 516, and 1223", Astron. Astrophys. Suppl. Ser. 146, 471-479.
- Pfleiderer, J., Pfleiderer, M. and Hanslmeier (1987), "Photoelectric Five-Colour Photometry of the Asteroids, 16 Psyche, 201 Penelope and 702 Alauda", Astron. Astrophys. Suppl. Ser. 69, 117-122.
- Surdej, J., Louis, B., Cramer, N., Rufener, F., Waelkens, C., Barbier, R. and Birch, P.V. (1983), "Photoelectric Lightcurves and Rotation Period of the Minor Planet 201 Penelope", Astron. Astrophys. Suppl. Ser. 54, 371-378.
- Torppa, J., Kaasalainen, M., Michalowski, T., Kwiatkowski, T., Kryszczyńska, A., Denchev, P. and Kowalski, R. (2003), "Shapes and Rotational Properties of Thirty Asteroids from Photometric Data", Icarus 164, 346-383.
- Vannmunster, T. (2006), Peranso Period Analysis Software, Peranso Version 2.31, CBA Belgium Observatory.
- Wang, X.-B. (2002), "CCD Photometry of Asteroids (58) Concordia, (360) Carlova and (405) Thia", Earth, Moon, and Planets 91, 25-30.
- Wang, X.-B. and Zhang, X.-L. (2006), "Determination of Rotational Parameters of Asteroid (360) Carlova", Chinese Astron. Astrophys. 30, 410-419.
- Warner, B.D. (2010), MPO Software, Canopus version 10.3.0.2, Bdw Publishing, Colorado Springs, CO.

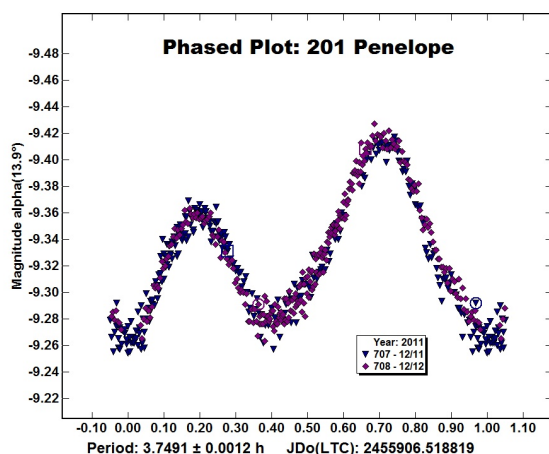


Figure 1
Folded light curves (phase vs relative flux) from the 2011 photometric campaign of 201 Penelope

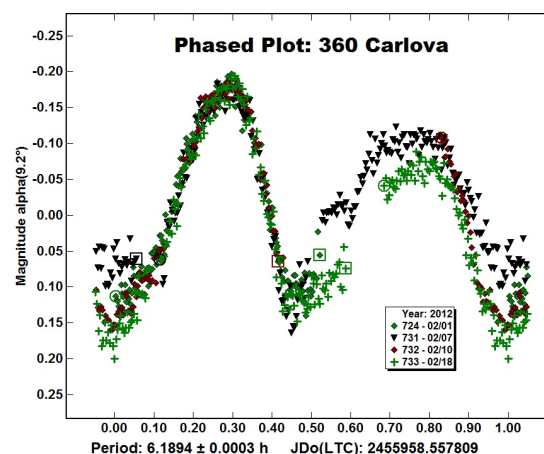


Figure 2
Folded light curves (phase vs relative flux) from the 2012 photometric campaign of 360 Carlova

Three Color CCD Monitoring of the Supernova SN 2012aw

Abstract

CCD images of SN 2012aw were acquired in B, V, and R passbands between March and May 2012. Analysis of the light curves during this period of time was consistent with reports that SN 2012aw is a type IIP supernova .

1. Introduction

This supernova initially named PSN J10435372+1140177 is positioned 60" west and 115" south of the center of M95 in an outer spiral arm. While at Rmag 15, SN 2012aw was first detected by Paolo Fagotti of the Italian Supernova Search Project on March 16, 2012 and continues to be monitored world-wide. As suggested by its location in a star forming outer region of a galaxy, it was determined to be a type IIP supernova by observations from the Swift satellite observatory (Brown 2012). A plateau of almost constant R brightness between mag 13-13.5 continues to be observed well into June, 2012.

2. Methods, Observations and Data Reduction

2.1 Astrometry

Images of SN 2012aw were matched against the UCAC3-based standard star fields provided in MPO Canopus (V10.3.0.2 Bdw Publishing, Inc.). This "automatch" feature generates a star chart centered on the putative center of the image and then matches the chart's center, rotation, and scaling to the image. Plate constants are internally calculated which convert X/Y coordinates of a detected object to a corresponding RA and declination.

2.2 Photometry

CCD observations at UnderOak Observatory span from March 22, 2012 to May 11, 2012. Equipment included a 0.2-m catadioptric telescope with an SBIG ST8-XME CCD camera mounted at the primary focus. The KAF 1603ME camera array (1530×1020) comprised of square pixels (9 μ m) produces a $\sim 14 \times 21$ arcmin field-of-view (FOV) with an image scale of ~ 1.6 arcsec/pixel with this optical assembly (Figure 1). The CCD camera was maintained at -15°C with thermoelectric cooling. Binned (2x2) multi-bandwidth (B, V, and R) imaging was performed with Custom Scientific photometric filters manufactured to match the Johnson-Cousins-Bessell prescription. During each session, images (≥ 6) in each bandpass were sequentially collected every 60-90s; data acquisition and reduction (raw lights, darks, and flats) for this camera system has been described elsewhere (Alton 2010). Instrumental readings were reduced to AAVSO-based magnitudes using the MPOSC3 reference star fields built into MPO Canopus.

3. Results and Discussion

3.1 Ensemble Photometry

Three comparison stars in the same field of view with SN 2012aw (Table 1) were used to calculate the relative change in flux and AAVSO-derived standard magnitudes (AAVSO Chart No. 6986RE) . During the entire campaign the airmass ($\text{Alt} > 30^\circ$) for all observations was kept under 2 to minimize error due to differential refraction and color extinction.

MPOSC3 ^a Star Identification	R.A.	DEC	MPOSC3 B mag	MPOSC3 V mag	MPOSC3 R mag
V. SN 2012aw	10 ^h 43 ^m 53.735 ^s	11°40'17.63" ^b	13.48 - 14.64 ^c	13.24 - 13.49	12.99 - 13.22
C ₁ . MPO3J10433923+1144197	10 ^h 43 ^m 39.23 ^s	11°44'19.7"	13.24 (12.97) ^d	12.16 (11.95)	11.57 (11.38)
C ₂ . MPO3J10432494+1145189	10 ^h 43 ^m 24.91 ^s	11°45'18.9"	13.63 (13.48)	12.88 (12.77)	12.46 (12.32)
C ₃ . MPO3J10433080+1149510	10 ^h 43 ^m 30.80 ^s	11°49'51.0"	11.70 (11.70)	11.25 (11.23)	10.98 (10.89)
a: MPOSC3 is a hybrid assemblage which includes a large subset of the Carlsberg Meridian Catalog (CMC-14) as well as from the Sloan Digital Sky Survey (SDSS). b: RA and DEC from Henden et al 2012 c: Range of magnitudes in light curves collected at UO between 22Mar2012 and 11May2012 d: AAVSO comparison star magnitudes in parenthesis					

Table 1. Astrometric coordinates (J2000) and MPOSC3 catalog magnitudes (V, B and R) for SN 2012aw and three comparison stars used in this photometric study

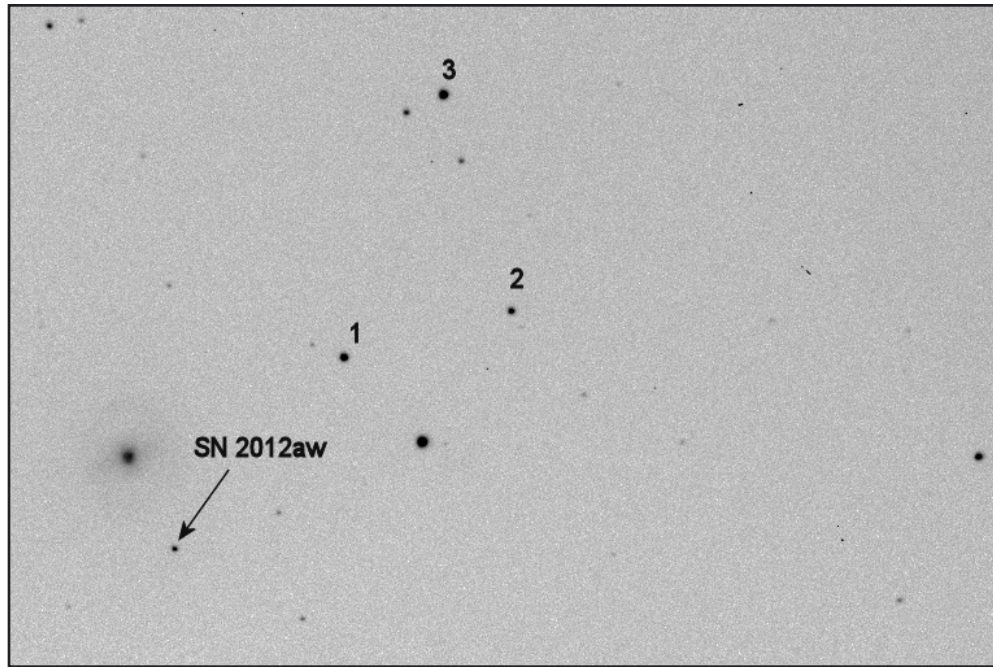


Figure 1. SN 2012aw image field of view (R-band) showing comparison stars used to determine AAVSO-based B, V and R magnitudes.

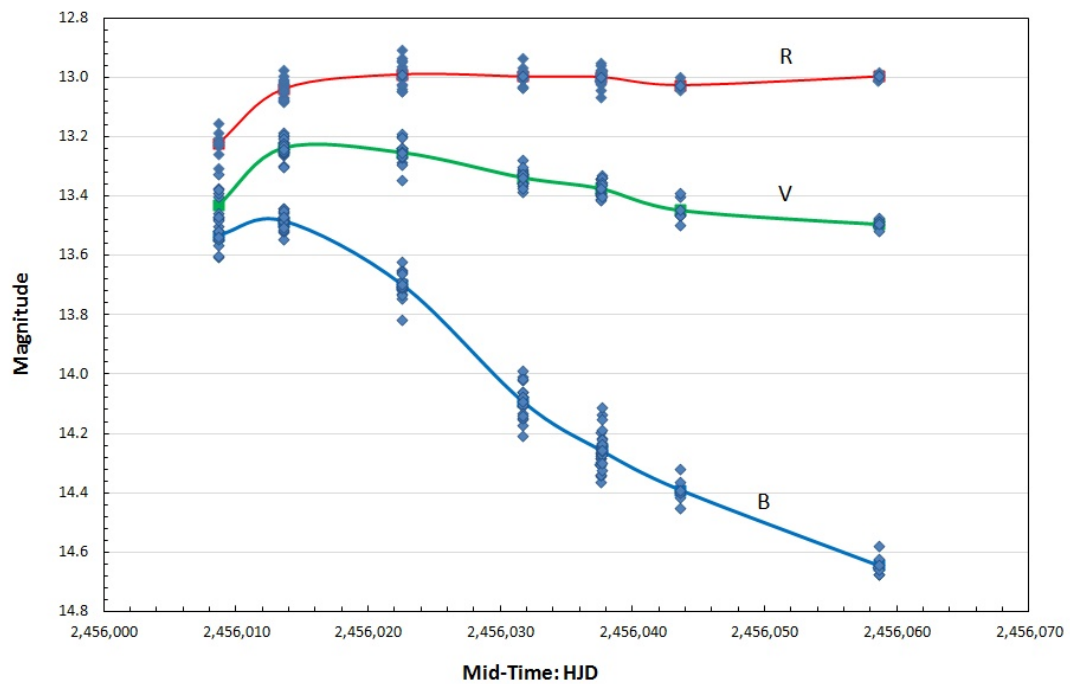


Figure 2. SN 2012aw lightcurve in B, V and R passbands between 22March and 11May2012.

3.2 Light Curve Analysis

Obvious differences in the lightcurve decay rate amongst the three filters (Figure 2) emerged by the third imaging session (5 April 2012). The more rapid decline in blue luminosity is not unexpected and portends the progressive reddening of SN 2012aw with time. This can also be visualized with the shift in color index (B-V and V-R) observed during this investigation (Figure 3). These data collectively suggest that SN2012aw has not yet finished the plateau stage of a type IIP supernova, however based upon other examples in the literature (Doggett and Branch 1985; Barbon et al 1979; Gurugubelli et al. 2008) a fairly precipitous drop in overall luminosity may occur fairly soon (100+ days after maximum light).

4. Conclusions

The fortuitous appearance of a relatively bright supernova during the early spring provided an exceptional opportunity to observe one of the most energetic phenomena that an amateur astronomer can witness. Photometric multi-color (B, V and R) data collected from SN2012aw at UnderOak Observatory between March and May 2012 corroborate other published findings which indicate that this is a type IIP supernova.

5. References

- Alton, K.B. 2010, JAAVSO 38.
 Barbon, R., Ciatti, F. & Rosino, L. 1979, Astron. Astrophys, 72, 287.
 Brown, P.J. 2012, The Astronomer's Telegram, 3979.
 Doggett, J.B. & Branch, D. 1985, AJ, 90, 2303.
 Gurugubelli, U.K., Sahu, D.K., Anupama, G.C. & Chakradhari, N.K. 2008, Bull. Astr. Soc. India, 36, 79.
 Henden, A., Kracji, T & Munari, U. 2012, IBVS, 6024.

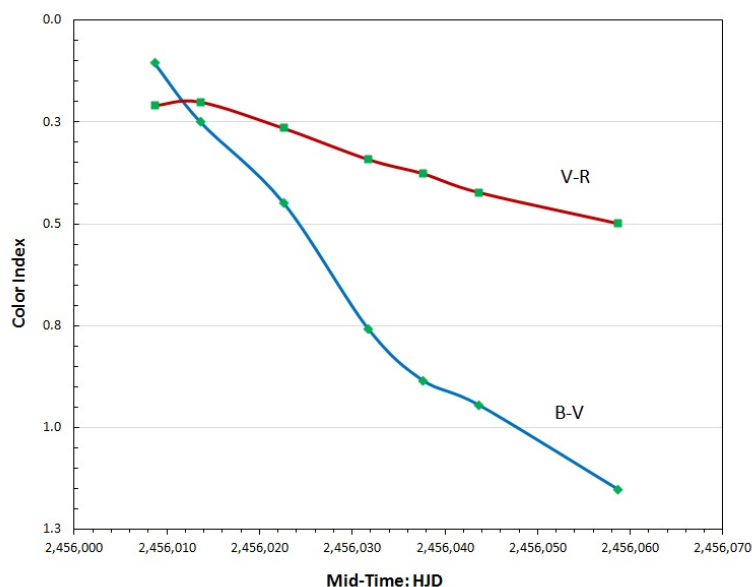


Figure 3. SN 2012aw reddening between 22 March and 11 May 2012.

Caveats:

The "UnderOak Observer" is published advertisement free using Scribus (v1.3.3.14). Its intent is both entertainment and informational. Every reasonable effort is made to verify facts and avoid personal bias, however, the reader bears full responsibility for actually believing what I have written.

Cover Page Art:

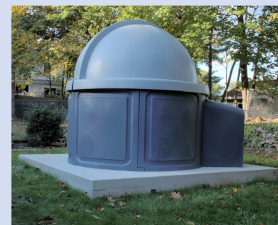
NGC 6914 is a blue reflection nebulae in Cygnus. Color was rendered using Registrar after synthesizing green from red and blue images downloaded with the DSS Plate Finder (http://archive.stsci.edu/cgi-bin/dss_plate_finder).

Editor: Kevin B. Alton

Writer: Kevin B. Alton

Public Access:

Free access to any light curve data associated with research published in the UO can be obtained by request (mail@underoakobservatory.com)



Research Article

A Fresh Look at the Algol-like Eclipsing Binary AO Ser

Kevin B. Alton
UnderOak Observatory
70 Summit Ave., Cedar Knolls, NJ 07927
mail@underoakobservatory.com

Andrej Prša
Dept. of Astronomy & Astrophysics
Villanova University
800 Lancaster Ave., Villanova, PA 19085
aprsa@villanova.edu

The following report was recently presented at the 2012 Symposium on Telescope Science in Big Bear Lake, CA and will be published as part of their Proceedings at a later date. This meeting was particularly eventful since it included the combined membership from the Society for Astronomical Sciences (SAS) and the American Association of Variable Star Observers (AAVSO). It was an especially rewarding experience to be invited and then have the opportunity to network with astronomers who have like-minded interests. As is certainly the case with this article, many other presentations involved the collaborative effort of professional and amateur astronomers. Aside from Dr. Prsa's extremely active involvement with the Kepler Mission, my co-author is also the author of PHOEBE, a user-friendly interface to the Wilson-Devinney code used to model light curves from eclipsing binary stars. Without his mentorship it would not have been possible to put together this comprehensive study of AO Serpentis.

Abstract

CCD images acquired in B, V, and I_c passbands between July and August 2008 and from June to August 2010 were used to revise the ephemeris and update the orbital period for AO Ser. Analysis of the O-C diagram using all available time-of-minima data revealed a continually increasing orbital period for at least 68 years. Thereafter, a sudden decrease in orbital period (~ 0.84 sec) most likely occurred during the first few months of 1998; potential causes for this abrupt jump and other alternating changes in period are discussed. Although the spectral classification of the primary star has been long been considered A2V (Teff ~ 8800 K), B-V data from this study as well as color index estimates from several other recent survey catalogs suggest a significantly cooler A7V (Teff ~ 7800 K) primary. A semi-detached Roche model

of the binary produced theoretical fits matching light curve data in all passbands. AO Ser is reported to be an oscillating Algol-type variable star referred to as an oEA system. Using Fourier methods, lightcurve analysis in this study did not convincingly reveal any underlying periodicity other than that expected from the dominant orbital period.

1. Introduction

AO Ser is a short period (< 1 day) and bright Algol-type binary suitable for study by amateur and professional astronomers alike. After its discovery in 1935 by the prolific observer Cuno Hoffmeister, the publication record for AO Ser was very sporadic with only a handful of times-of-minima (ToM) available for each of the next three decades. These mostly included photographic as well as visual timings. Only since 1969 has a steady flow of ToM values been available but no full light curve had been published until Zavros et al. (2008). AO Ser not only varies extrinsically by mutual eclipses but evidence is mounting that it also varies intrinsically by δ Sct-type pulsation of its primary component (Kim et al. 2004; Zavros et al. 2008). This new class of oscillating Algol-type variable stars is now designated as an oEA variable (Mkrtychian et al. 2004). More recently, the multiband (V and R) photometric properties and period variations of AO Ser were published by Yang et al (2010).

AO Ser (BD+17°2943) varies in magnitude (V) between 10.8 and 12.2; the first modern orbital period (0.87934745 d) was reported by Koch (1961). This target is favorably positioned ($\alpha_{J2000} = 15^h 58^m 18^s.408$, $\delta_{J2000} = +17^\circ 16' 9.96''$) for mid-latitude backyard observers in the Northern Hemisphere with a clear view of Serpens Caput. Its spectral type (A2) reported by Brancewicz & Dworak (1980) is consistent with what would be expected for an Algol-like binary system, however, evidence from this study and several survey catalogs (eg. Tycho-2, USNO-A2.0, USNO-B1.0, and 2MASS) suggest a much cooler A7 system. This difference from all other published reports on this binary system will be discussed herein.

2. Methods, Observations and Data Reduction

2.1 Astrometry

Images of AO Ser were matched against the UCAC3-based standard star fields provided in MPO Canopus (V10.3.0.2 Bdw Publishing, Inc.). This “automatch”

feature generates a star chart centered on the putative center of the image and then matches the chart's center, rotation, and scaling to the image. Plate constants are internally calculated which convert X/Y coordinates of a detected object to a corresponding RA and declination.

2.2 Photometry

CCD observations at UnderOak Observatory span from July 25, 2008 to August 22, 2008 and then again from June 19, 2010 to August 31, 2010. Equipment included a 0.2-m catadioptric telescope with an SBIG ST 402ME CCD camera mounted at the primary focus. The KAF 0402ME camera array (765×510) comprised of square pixels (9 μm) produces a $\sim 9 \times 14$ arcmin field-of-view (FOV) and an image scale of ~ 1 arcsec/pixel with this optical assembly. The CCD camera was maintained at 0°C with thermoelectric cooling. Automated multi-bandwidth (B, V, and I_c) imaging was performed with SBIG photometric filters manufactured to match the Bessell prescription. During each 2008 session, an image in each bandpass was sequentially collected every 45 s; data acquisition and reduction (raw lights, darks, and flats) for this camera system has been described elsewhere (Alton 2010). The other campaign which started in 2010 employed essentially the same equipment except that the acquisition time for each filter was increased to 60 s. Instrumental readings were reduced to catalog-based magnitudes using the MPOSC3 reference star fields built into MPO Canopus. The MPO Star Catalog (MPOSC3) is a hybrid assemblage which includes a large subset of the Carlsberg Meridian Catalog (CMC-14) as well as from the Sloan Digital Sky Survey (SDSS). Almost all stars in MPOSC3 also have $\text{BVR}_c I_c$ magnitudes derived from 2MASS J-K magnitudes; these have an internal consistency of ± 0.05 mag for V, ± 0.08 mag for B, ± 0.03 mag for I_c , and ± 0.05 mag for B-V (Warner 2007).

2.3 Lightcurve Analyses

Light curve modeling was performed using Binary Maker 3 (Bradstreet & Steelman 2002) and PHOEBE 0.31a (Prša & Zwitter 2005) both of which employ the Wilson-Devinney (W-D) code (Wilson & Devinney 1971; Wilson 1979). Geometric renderings were produced by Binary Maker 3 (Bradstreet & Steelman 2002).

3. Results and Discussion

3.1 Ensemble Photometry

Five comparison stars in the same field of view with AO Ser were used to calculate the relative change in flux and standard magnitudes (Table 1). Over the duration of each session, comparison stars did not exhibit any variable behavior so Comp Cavg values remained constant over each observation period (Figure 1). The

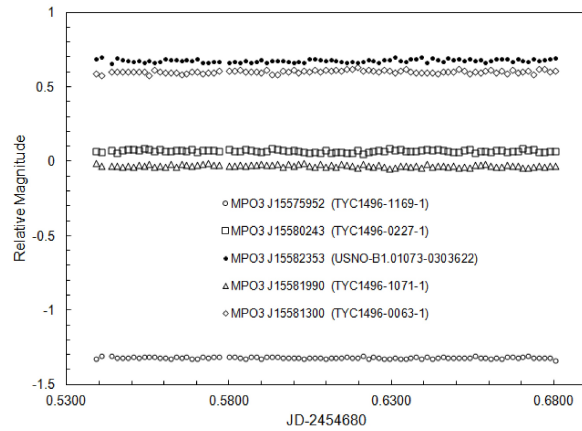


Figure 1. Constant relative magnitude (I_c -band) exhibited by comparison stars during a typical AO Ser photometric session

mean standard magnitude for each comparison star varied between ± 0.015 (V and I_c) and ± 0.03 (B) mag.

During the entire campaign the airmass for all observations was kept under 2 to minimize error due to differential refraction and color extinction.

3.2 Folded Light Curves and Ephemerides

Individual photometric values in B ($n=1573$), V ($n=1598$), and I_c ($n=1580$) were combined by filter to produce light curves that spanned 4 weeks of imaging in 2008 and 10 weeks in 2010. A period solution from all folded 2008 and 2010 datasets was calculated by MPO Canopus.

Accordingly, the linear ephemeris equation (1) for the heliocentric primary minimum was initially determined to be:

$$\begin{aligned} \text{Min } I &= \\ \text{HJD}2454664.54963 + 0.8793429 (\pm 0.0000013) \cdot E \end{aligned} \quad (1)$$

This result is in general agreement with the orbital period reported over the past 5 decades from other investigators.

The period determination was confirmed with periodograms produced (Peranso v 2.1, CBA Belgium Observatory) by applying periodic orthogonals (Schwarzenberg-Czerny 1996) to fit observation and analysis of variance (ANOVA) which was used to evaluate fit quality. ToM values were estimated by Minima (V24b, Nelson 2007) using a simple mean from a suite of six different methods including parabolic fit, tracing paper, bisecting chords, Kwee & van Woerden (1956), Fourier fit, and sliding integrations (Ghedini 1981). Four new secondary (s) and two new primary (p) minima were detected during this investigation. Since no obvious color dependencies emerged, the timings from all three

MPOSC3 ^a Star Identification	RA	DEC	B mag	V mag	I _c mag	(B-V)
MPO3 J15575952	15 ^h 57 ^m 59 ^s .52	+17°19'26.3"	10.843	10.41	9.889	0.433
MPO3 J15580243	15 ^h 58 ^m 02 ^s .43	+17°21'13.4"	11.985	11.547	11.021	0.438
MPO3 J15581300	15 ^h 58 ^m 13 ^s .00	+17°16'42.5"	12.852	12.158	11.391	0.694
MPO3 J15581841	15 ^h 58 ^m 18 ^s .41	+17°16'10.0"	11.667	11.208	10.661	0.459
MPO3 J15581990	15 ^h 58 ^m 19 ^s .90	+17°19'45.4"	12.518	11.50	10.445	1.018
MPO3 J15582353	15 ^h 58 ^m 23 ^s .53	+17°18'39.8"	12.876	12.214	11.474	0.662
a: MPOSC3 is a hybrid assemblage which includes a large subset of the Carlsberg Meridian Catalog (CMC-14) as well as from the Sloan Digital Sky Survey (SDSS).						

Table 1. Astrometric Coordinates and Estimated Color of AO Ser (MPO3 J15581841) and Five Comparison Stars in Same Field of View

filters were averaged for each newly determined ToM.

Residual values (O-C) were estimated from a complete set of visual (vis), photographic (pg), photoelectric (pe) and CCD timings reported over the past 80 years.

Calculations were initially based upon the linear elements (2) defined by Kreiner (2004):

Min I =

$$\text{HJD}2452500.3991(\pm 0.0007) + 0.8793410(\pm 0.0000004) \cdot E \quad (2)$$

The O-C diagram (Figure 2) for AO Ser is complex and characterized by parabolic and possibly alternating changes exhibited by many other late type Algol-like binary systems such as U Cep (Manzoori 2008), Y Leo (Pop 2005), TY Peg (Qian 2002), and X Tri (Qian 2002).

Regression analysis using a scaled Levenberg-Marquardt algorithm (Press et al.1992) as implemented in QtiPlot (v0.9.8 2010) revealed that the O-C data from the initial timing in 1930 until the last twelve years could be fit ($r^2 > 0.99$) by a quadratic expression (3) modulated with a sinusoidal term as follows:

$$c + a_1x + a_2x^2 + a_3\sin(a_4x + a_5) \quad (3)$$

Accordingly, the coefficients (\pm error) for each solved term in the above equation (3) are provided in Table 2.

From the parabolic component ($c + a_1x + a_2x^2$) it is apparent that the orbital period has been slowly and linearly increasing with time as suggested by the positive coefficient (a_2) for the quadratic term, x^2 . Algol-type binaries typically consist of a hot main-sequence massive primary well within its Roche lobe and a less-massive subgiant companion filling its Roche lobe. Gas streams from the secondary to the primary result in mass exchange and barring any other competing phenomena, the net effect is a change in the orbital period. In this case, the orbital period rate of increase ($\Delta p/p = 2a_2 = 1.25 \times 10^{-10}$) of this system, which is equivalent to a period increase rate of $dp/dt = +0.004479 \text{ sec } y^{-1}$, lasted for at least 68 years but suddenly slowed to a standstill as judged by the break in O-C residuals (Figure 2) around cycle -1855. The intersection of Q+S and L1 suggests this change which is centered at the beginning of 1998 probably occurred sometime between mid 1996 and mid-

Curve	c	a ₁	a ₂	a ₃	a ₄	a ₅
L1 ^a	1.593×10^{-3} ($\pm 0.290 \times 10^{-3}$)	-8.679×10^{-7} (± 0.228)	-	-	-	-
L2 ^a	-6.503×10^{-3} ($\pm 1.088 \times 10^{-3}$)	3.046×10^{-6} ($\pm 0.4189 \times 10^{-6}$)	-	-	-	-
Q+S ^b	1.667×10^{-2} ($\pm 0.136 \times 10^{-2}$)	$+8.911 \times 10^{-6}$ ($\pm 0.237 \times 10^{-6}$)	$+6.240 \times 10^{-11}$ ($\pm 0.760 \times 10^{-11}$)			
Q+S ^c	1.667×10^{-2} ($\pm 0.136 \times 10^{-2}$)	$+8.911 \times 10^{-6}$ ($\pm 0.237 \times 10^{-6}$)	$+6.240 \times 10^{-11}$ ($\pm 0.760 \times 10^{-11}$)	$+3.748 \times 10^{-3}$ ($\pm 0.593 \times 10^{-3}$)	4.249×10^{-4} ($\pm 0.206 \times 10^{-4}$)	3.209 (± 0.244)
a: Linear least squares fit: (O-C) = $c + a_1x$ b: Non-linear regression fit (O-C) = $c + a_1x + a_2x^2$ c: Non-linear regression fit (O-C) = $c + a_1x + a_2x^2 + a_3\sin(a_4x + a_5)$						

Table 2. Coefficients (\pm error) From Regression Analysis of O-C vs Cycle Number Data for AO Ser

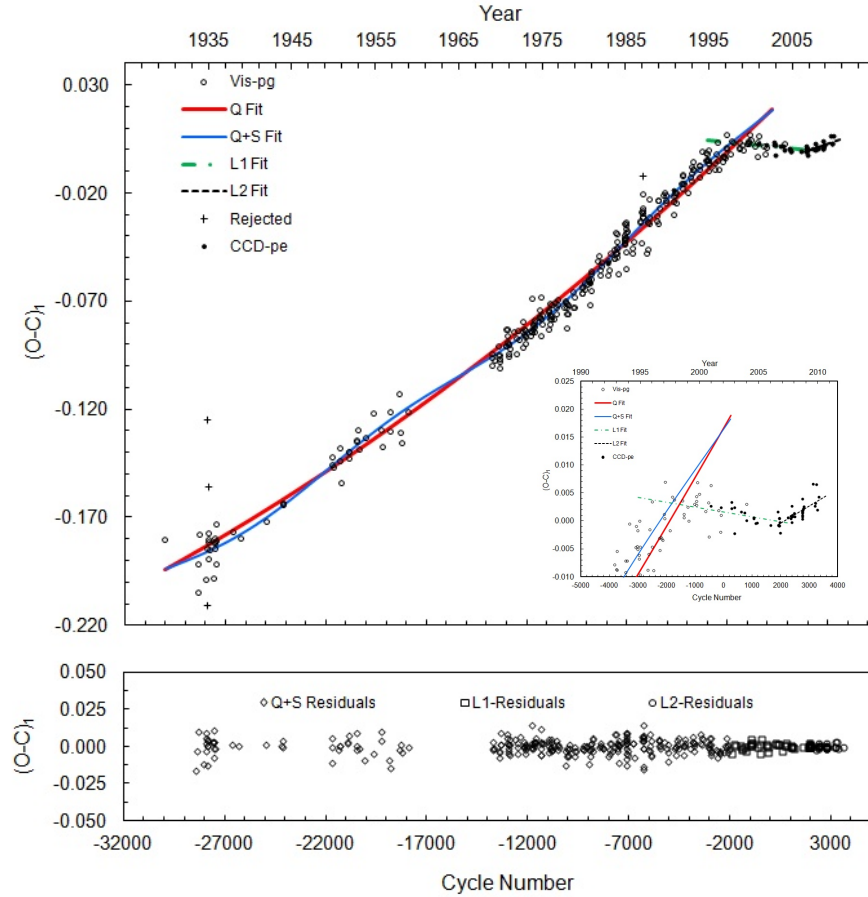


Figure 2. Nonlinear quadratic+sine term fit (Q+S) of residuals (O-C) vs cycle number for AO Ser observed from March 1930 to 17June1998. The inset figure shows a breakpoint centered near cycle -1855 (Feb-March 1998) and the straight line linear fit of data (L1) through cycle 1983.5 (mid 2007). Near term data (L2) were also fit using simple linear least squares analysis. The bottom panel represents a composite plot of all (O-C)₂ residuals from fitting Q+S, L1, and L2. All ToM values and references used to prepare this figure can be obtained by request (mail@underoakobservatory.com).

1999. This cannot be attributed to the shift from vis-pg to ccd-pe recordings since instrument-derived ToMs regularly reported after cycle 118.5 continue in a similar fashion until another break is observed near cycle 2000. This characterization of AO Ser is in contrast to that described by Yang et al. (2010) who only report a period decrease since 1981. This obvious difference from our findings is discussed further on in this section along with the potential for a light time effect which they also had proposed. Calculations based on linear coefficients from the quadratic + sine term (4) and simple least squares (5) fits resulted in the following ephemerides, respectively:

$$\text{Min I} = \text{HJD}2,455,666.9548(\pm 0.0013) + 0.8793499(\pm 0.0000002) \cdot E \quad (4)$$

$$\text{Min I} = \text{HJD}2,455,666.9045(\pm 0.0003) + 0.8793401(\pm 0.0000002) \cdot E \quad (5)$$

The orbital period difference (-9.7788×10^{-6} days) between equations (4) and (5) corresponds to a rather large decrease (0.844 sec) over a relatively short period of time. The two most likely causes for a decrease in period are mass exchange between the components and/or angular momentum loss from the binary system. A rate of conservative mass transfer can be predicted (6) as follows from Kwee (1958):

$$dm/dt = m \left[\frac{q}{3P(1-q^2)} \right] dP/dt \quad (6)$$

where

$$m = M_1 + M_2 \text{ and } q = M_2/M_1$$

The abrupt change in orbital period likely took place within a 3 year window as suggested by the O-C diagram (Figure 2). Assuming the solar mass of a putative A7V primary approximates $1.82 M_{\text{sol}}$ (Harmanec 1988), then from the mass ratio ($q_{\text{ph}}=0.235$) determined herein, the calculated mass loss is $6.851 \times 10^{-7} M_{\text{sol}} \text{ y}^{-1}$. Averaged over three years this translates into nearly two-thirds of the Earth's mass. Alternatively from Mikuž et al. (2002),

the associated change in angular momentum can also be estimated (7) from the equations for total angular momentum (L) and Kepler's law:

$$\frac{dL}{L} = \left[\frac{2}{3} + \frac{q}{3(1+q)} \right] dm_1/m_1 + \left[1 - \frac{q}{3(1+q)} \right] dm_2/m_2 + \frac{1}{3} dP/P, \quad (7)$$

where $q = m_2/m_1$ and P is the period of AO Ser. Assuming that the angular momentum change dL can only be zero or a negative value, then in order to produce

Time of Minimum (- 2,400,000)	Type	Cycle Number	(O-C) ₁	(O-C) ₂	Reference
54175.5429	p	1905	-0.000805	-0.000700	3
54186.5371	s	1917.5	0.001632	-0.000662	3
54201.4835	s	1934.5	-0.000765	-0.000610	3
54211.5959	p	1946	-0.000786	-0.000575	3
54213.3545	p	1948	-0.000868	-0.000569	3
54220.3893	p	1956	-0.000826	-0.000545	2
54220.3906	p	1956	0.000494	-0.000545	2
54224.7859	p	1961	-0.000901	-0.000529	1
54242.3741	p	1981	0.000459	-0.000469	2
54244.5717	s	1983.5	-0.000274	-0.000461	3
54491.6646	s	2264.5	-0.002195	0.000395	4
54574.7651	p	2359	0.000581	0.000683	5
54581.3604	s	2366.5	0.000823	0.000706	6
54599.3865	p	2387	0.000433	0.000768	7
54610.8172	p	2400	-0.000300	0.000808	5
54612.5770	p	2402	0.000818	0.000814	8
54614.3375	p	2404	0.002636	0.000820	8
54628.4051	p	2420	0.000780	0.000869	8
54685.5625	p	2485	0.001015	0.001067	9
54696.5546	s	2497.5	0.001353	0.001105	9
54926.5017	p	2759	0.000781	0.001901	10
54928.2612	p	2761	0.001599	0.001907	11
54928.2614	p	2761	0.001799	0.001907	11
54929.1397	p	2762	0.000758	0.001911	11
54929.1400	p	2762	0.001058	0.001911	11
54932.2170	s	2765.5	0.000364	0.001921	11
54932.2181	s	2765.5	0.001464	0.001921	11
54939.6925	p	2774	0.001466	0.001947	12
54952.8851	p	2789	0.003951	0.001993	13
54968.7113	p	2807	0.002013	0.002048	12
54974.4272	s	2813.5	0.002196	0.002067	9
55259.7737	p	3138	0.002542	0.003056	14
55316.4953	s	3202.5	0.006647	0.003252	15
55327.4831	p	3215	0.002685	0.003290	15
55366.6142	s	3259.5	0.003157	0.003426	9
55395.6358	s	3292.5	0.006504	0.003526	9
55436.5206	p	3339	0.001938	0.003668	9
55666.9103	p	3601	0.004259	0.004466	16
(1) Baldwin & Samolyk 2007 (2) Brát <i>et al.</i> 2007 (3) Borkovits <i>et al.</i> 2008 (4) Parimucha <i>et al.</i> 2009 (5) Samolyk 2008 (6) Brát <i>et al.</i> 2008 (7) Hübscher <i>et al.</i> 2010 (8) Lampens <i>et al.</i> 2010 (9) Present study (10) Doğru <i>et al.</i> 2009 (11) Yang <i>et al.</i> 2010 (12) Samolyk 2010 (13) Diethelm 2009 (14) Samolyk 2011 (15) Doğru <i>et al.</i> 2011 (16) Diethelm 2011					

Table 3. Near Term Recalculated Residuals (O-C)₂ for AO Ser Following Simple Linear Least Squares Fit of (O-C)₁ and Cycle Number Between 2007March16 and 2011April15.

a period change of $dP/P=1.11 \times 10^{-5}$ the total mass lost from the system had to be at least 3.23×10^{24} kg or slightly more than one half (~54%) of Earth's mass. The corresponding magnitude of mass loss estimated by either equation 6 or 7 is significant but nonetheless not unprecedented (1.626×10^{-4} to $9.5 \times 10^{-8} M_{\text{sol}} \text{ y}^{-1}$) for semi-detached binaries (van Rensbergen et al. 2011).

Due to the continually changing nature of the O-C diagram, a new ephemeris equation (8) based upon a linear least squares fit (L2) of near-term data (Table 3) collected over the past four years (cycle 1905 to 3601) was calculated:

$$\text{Min I} = \text{HJD } 2,455,666.9105 (\pm 0.0011) + 0.8793441 (\pm 0.0000004) \cdot E \quad (8)$$

As such, if the complex O-C behavior of this system continues unabated, revised ephemerides for AO Ser will need to be calculated on a more regular basis. The composite residuals from the quadratic + sine term fit (Q+S) and simple least squares fit (L1 and L2) are shown in the bottom panel of Figure 2. No additional underlying periodicity in the (O-C)₂ diagram was uncovered with Peranso using Fourier (Lomb Scargle) and statistical (ANOVA) methods. In a recent publication, Yang et al. (2010) attempted to make a case for decreasing period and a third body with an incomplete set of data which excluded all pg and visual (n=300) plus other CCD readings (n=10) published from 1941 through the middle of 2008. It is unfortunate that this rich set of data was not considered since out of 300 additional visual and pg observations, we found that only four values needed to be rejected as spurious. In contrast when all data are evaluated, residuals for the first seven decades clearly describe an upwardly turned parabola (Q), namely behavior consistent with conservative mass transfer and a continually increasing period. Additionally on this quadratic curve, there is evidence for underlying cyclical changes based upon non-linear regression analysis (Equation 3). The amplitude (0.003748 ± 0.000593 d) of the periodic oscillation is defined by a_3 , the coefficient of the sine term. Assuming for the moment that this behavior is associated with a third body, then according to the relationship:

$$P_3 = 2\pi P / \omega,$$

where the angular frequency, ω , corresponding to $a_4 = 4.249 (\pm 0.206) \times 10^{-4}$, its Keplerian orbital period would be ~36 y. This estimate is more than twice as long as the periodic value (~17 y) reported by Yang et al (2010) using an incomplete dataset covering the time span between

1981 and 2009. Analysis of the complete set O-C residuals available between 1930 and 2011 paints a very different behavioral picture for this binary system. We agree there is a modicum of evidence that suggests cyclic, if not sinusoidal behavior in the O-C diagram but only up to 1998. Thereafter, between 1998 and 2011 the O-C trace is curvilinear but not necessarily sinusoidal for this system. It is possible that the event(s) responsible for the sudden change in orbital period in 1998 have masked our ability to tease out the putative 36 y periodicity observed during prior epochs. Nonetheless, since the gravitational influence of a third body cannot be simply turned off, we believe that evidence for the presence of a third body in this system is inconclusive. Moreover, during attempts to fit light curve data to a Roche type model with our data, neither the orbital eccentricity (e) nor third light (l_3) rose above a level different than zero when included as variable parameters. This begs the question as to what other phenomena might lead to cyclic, but not necessarily, persistent sinusoidal behavior. Hall (1989) noted that Algol-like systems which exhibit alternating variability in their O-C diagrams are almost exclusively those possessing a late-type secondary which to a high degree of certainty are chromospherically active.

Furthermore, earlier type Algols composed of two radiative-envelope companions yield much simpler O-C diagrams rarely demonstrating cyclic behavior (Budding & Demircan 2007). The secondary in AO Ser is likely a rapidly rotating late type subgiant and therefore possesses a dynamically active lobe-filling convection envelope. A plausible alternative to the light travel time effect (LITE) from additional unseen mass involves cyclic variability arising from magnetic activity of the secondary (Applegate 1992). In addition, Biermann & Hall (1973) proposed a model where the secondary experiences abrupt episodes of mass transfer which orbits the primary as a disk. This leads to a temporary reservoir of orbital angular momentum where P decreases but at later time, angular momentum is returned by accretion during which P increases. This scenario may have played out with AO Ser starting with the sudden break observed in the O-C diagram in early 1998 followed by a period decrease which begins to reverse direction around cycle 2000 (mid-2007). At this time in the absence of any supporting data from a spectroscopic study or speckle interferometry it would be speculative to assign any single reason or combination of phenomena that would unequivocally include LITE as an explanation to this very complex O-C diagram for AO Ser.

3.3 Light Curve Synthesis

Folded light curves (Figure 3) comprised of all observations (relative magnitude) in B, V, and I_c, show

that minima are separated by 0.5 phase. Collectively, mode 5 (semi-detached; secondary fills Roche lobe), synchronous rotation and circular orbits were selected for modeling by PHOEBE. Each model fit incorporated individual observations assigned an equal weight of 1.

Bolometric albedo ($A_1=1$) and gravity darkening coefficients ($g_1=1$) for the primary component were based on theoretical considerations for radiative stars reported by Eddington (1926) and von Zeipel (1924), respectively. As mentioned previously, third light (l_3) did not rise above a value different than zero when adjusted.

Bolometric albedo ($A_2=0.5$) and gravity darkening coefficients ($g_2=0.32$) for cooler stars with convective envelopes were assigned as determined by Rucinski (1969) and Lucy (1967), respectively. After any change in Teff, logarithmic limb darkening coefficients (x_1, x_2, y_1, y_2) for both stars were interpolated from PHOEBE (Van Hamme 1993). Once an approximate fit was obtained, differential corrections (DC) were applied simultaneously to photometric data in all filters.

3.3.1 Binary Model

As mentioned earlier the spectral type reported by Brancewicz & Dworak (1980) was A2 while the color index ($B-V = -0.1$) listed by Kreiner et al (2004) suggests an even hotter primary star. Yet, evidence from this study which is the first to simultaneously acquire AO Ser light curves in B and V passbands, as well as data from multiple survey catalogs point to a much cooler system (Table 4). The B-V value (0.247) observed in this study was taken during Min II when spectral contamination by the secondary was least likely to bias the result. In addition, maximum galactic reddening ($E(B-V) = 0.0381$) in this region of the sky (Schlegel et al 1998) is unremarkable and therefore no adjustment has been made to obtain the associated intrinsic color index for AO Ser. On balance, we adopted an A7 spectral classification for AO Ser which is considerably cooler than that reported by all previous investigators; the effective temperature of the primary was estimated to be 7800 K based on the tables from Flower (1996). Values for q, Ω_1, Ω_2 , and i reported by Zavros et al. (2008) were used as a starting point for an unspotted fit (V bandpass) using Binary Maker 3. A_1, A_2, g_1, g_2, q , and T_1 were fixed

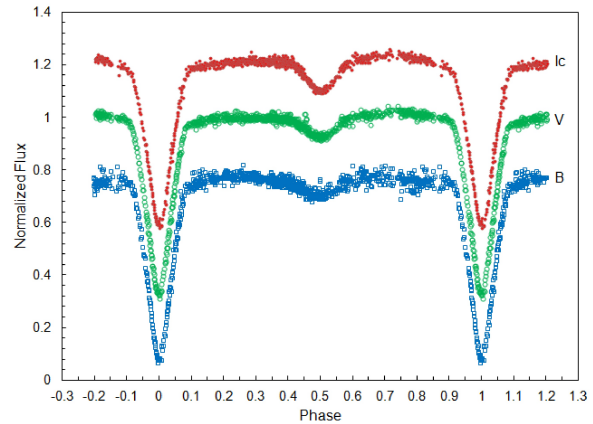


Figure 3. Folded (July - August 2008 and June - August 2010) CCD light curves for AO Ser captured in B, V, and I_C

parameters whereas Ω_1, T_2 , phase shift, x_1, x_2 , and i were iteratively adjusted until a reasonable fit of the observed relative flux by the model was obtained. Thereafter, the model fit was refined with PHOEBE while using DC to achieve a simultaneous minimum residual fit of all (B, V, and I_C) photometric observations. In mode 5, Ω_2 is constrained and as such is automatically calculated with any change to this parameter. The initial W D model fit was marginally acceptable in all passbands which led to further adjustment of variable parameters. Early investigators of this Algol like system had used a mass ratio ($q=m_2/m_1$) of 0.45, presumably based on a tabulation of computed parameters for eclipsing binaries published by Brancewicz & Dworak (1980). However, in the absence of any radial velocity data for this binary system, it was deemed appropriate to allow this physical element to also vary freely. An improved solution quickly emerged at a significantly different value, so it was decided to carefully examine this parameter under more controlled conditions. Mass ratio (q) was fixed over a range of 0.1 to 0.8 and a series of fits allowed to converge. The curve generated by plotting χ^2 as a function of the putative mass ratio showed a shallow minimum between $q=0.220$ and 0.260 (Figure 4). The mid point (0.240) was nominally assigned as the starting q -value during

Survey	Tycho-2	USNO-B1.0	USNO-A2.0	2MASS	ASCC-2.5 V3	Present Study
(B-V) ^a	0.219	0.195	0.235	0.459	0.266	0.247
Spectral Class ^b	A7	A7	A7	F5	A8	A7

a: Not corrected for galactic reddening – $E_{(B-V)} \sim 0.0381$
b: Estimated from Fitzgerald (1970)

Table 4. AO Ser Color Index (B-V) From Several Survey Catalogs and the Present Study

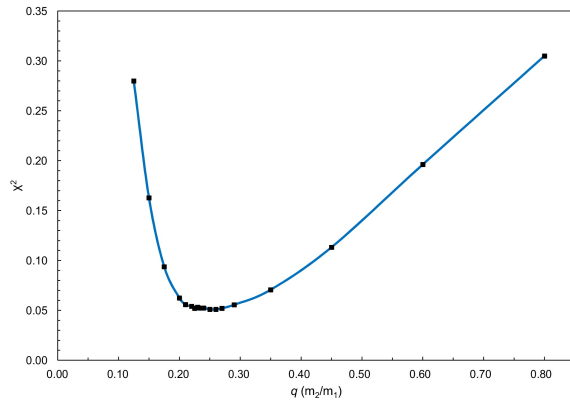


Figure 4. Search for mass ratio (q) providing the best simultaneous light curve fit (χ^2) using data from all passbands (B, V, and I_C). The shallow minimum is essentially the same between 0.22 and 0.26 q .

Roche modeling. Elements for AO Ser obtained using PHOEBE are provided in Table 5 while light curve fits for each filter band (B, V, and I_C) are respectively illustrated in Figures 5, 6, and 7. A 3 dimensional rendering produced using Binary Maker 3 depicts a spatial model for AO Ser (Figure 8). As might be expected from adopting an A7 primary for AO Ser instead of a hotter A2, most of the physical and geometric elements determined in this study are quite different from those most recently reported by Yang et al. (2010) and Zavros et al. (2008).

One other revealing difference is related to using a theoretical q value (0.45) from the literature (Zavros et al. 2008), as opposed to empirically determining a photometric q . As such, our value ($q_{ph}=0.235$) agrees

reasonably well with the value reported by Yang et al. 2010 ($q_{ph}=0.220$). Based upon a compilation of absolute dimensions of eclipsing binaries (Harmanec 1988), the mean stellar mass for an A7 main sequence binary star ($1.82 M_{sol}$) was used to estimate the mass of the secondary and the semi-major axis ($a=5.055$) in solar units. The associated mass ($0.428 M_{sol}$) of the secondary and best fit temperature for T_2 (4412 K; $\log 3.645$) of the putative sub-giant suggested a spectral type between K1 and K3 (Harmanec 1988, İbanoğlu et al. 2006, Surkova & Svechnikov 2004). Clearly, further spectroscopic analyses will be necessary to solidify the spectral classification of this Algol like system.

3.3.2 Oscillating Frequencies of the Primary Star

Recent evidence suggests that AO Ser not only varies extrinsically by mutual eclipses but also intrinsically by δ Sct-type pulsation of its primary component (Kim et al. 2004, Zavros et al. 2008). To this end, we investigated the possibility that such oscillation could be detected in our data. Frequency analysis by classical Fourier methods with Period04 (Lenz & Breger 2005) and Peranso did not convincingly expose any underlying periodicity other than that expected from the dominant orbital period. The spectral window (Figure 9) exhibits strong side-bands offset by 1 cycle per day and likely result from daily sampling aliases; results are shown for B=band, however, similar findings were observed in V and I_C . Data subsets intentionally stripped of measurements around the primary minimum or residuals remaining after Roche modeling were no more revealing of any underlying pulsations. Successive pre-whitening did not expose any other statistically meaningful ($s/n>4$) oscillations in the frequency range ($5-80 \text{ d}^{-1}$) expected for

Parameter	Present Study	Zavros <i>et al.</i> 2008	Yang <i>et al.</i> 2010
T_1 (K) ^a	7800	8770	9480
T_2 (K) ^b	4412 (33)	4858-5137 ^c	4786 (11)
q (M_2/M_1) ^b	0.235 (3)	0.45	0.220 (2)
A_1 ^a	1.0	1.0	1.0
A_2 ^a	0.5	0.5	0.5
g_1 ^a	1.0	1.0	1.0
g_2 ^a	0.32	0.32	0.32
Ω_1 ^b	3.56 (3)	4.625-4.936 ^c	2.597 (11)
Ω_2	2.318	2.778	2.282
i ^b	86.8 (4)	80.12-81.18 ^c	87.62 (17)

a: Fixed elements during DC
b: Error estimated from heuristic scanning of the $\Delta\chi^2$ surface (Prša and Zwitter 2005)
c: Range since V, R, and I not simultaneously fit during W-D modeling

Table 5. A Comparison of Selected Photometric Elements for AO Ser Obtained Following Roche Model Curve Fitting

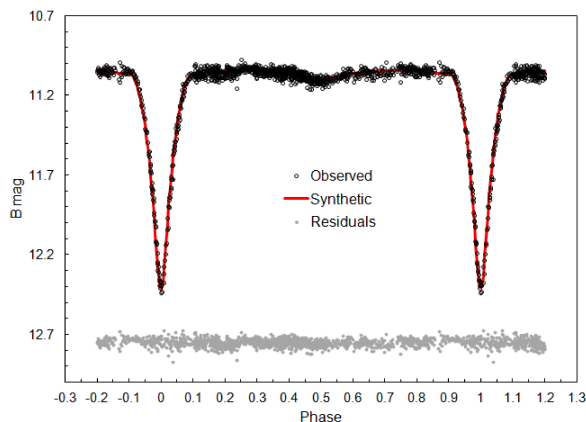


Figure 5. AO Ser light curve (B-band) synthesis determined by PHOEBE after simultaneous fit of all photometric data from three passbands (B, V, and I_C). Roche model residuals are adjusted by a fixed amount to display them in the same chart.

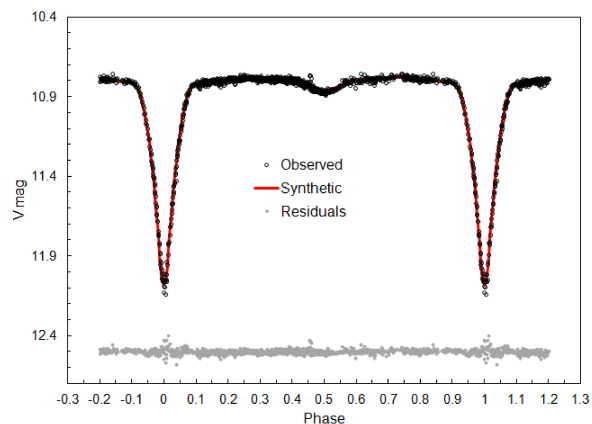


Figure 6. AO Ser light curve (V-band) synthesis determined by PHOEBE after simultaneous fit of all photometric data from three passbands (B, V, and I_C). Roche model residuals are adjusted by a fixed amount to display them in the same chart.

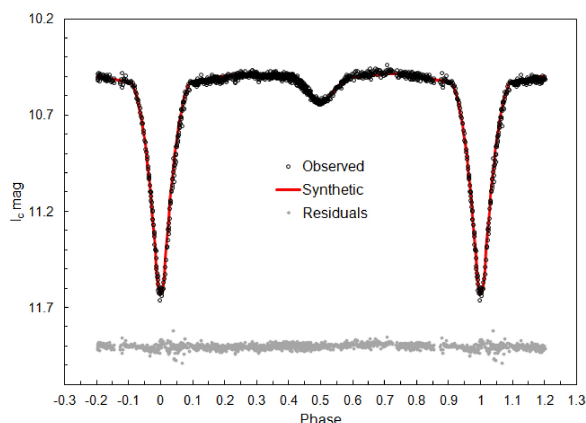


Figure 7. AO Ser light curve (I_C -band) synthesis determined by PHOEBE after simultaneous fit of all photometric data from three passbands (B, V, and I_C). Roche model residuals are adjusted by a fixed amount to display them in the same chart.

δ Sct-type pulsations (Breger 2000) according to the criterion proposed by Breger et al (1993). It is entirely possible, however, that intrinsic oscillations were not detected due to insufficient precision during photometric sampling given that low amplitude δ Sct-type pulsations may not exceed 0.06 mag (Christiansen 2007).

4. Conclusions

CCD (B, V, and I_C filters) photometric readings were used to revise the orbital period for AO Ser and calculate an updated ephemeris. A detailed period analysis using O-C residuals generated from observations spanning 80 years

revealed a very complex pattern of changes. Following at least seven decades of a constantly increasing orbital period, a sudden decrease (0.844 s) probably occurred around the beginning of 1998. Assuming no mass loss from the system and conservation of angular momentum,

On average the minimum amount of stellar material transferred during that period exceeded 50% the mass of Earth. Since then, the O-C residuals suggest that AO Ser is presently undergoing further changes caused by a yet to be determined phenomena or combination of effects.

Evidence points to cyclic, if not sinusoidal behavior in the O-C diagram but only up to 1998; however, this same cyclic periodicity (~ 36 y) is not obvious within subsequent O-C residuals available for this system between 1998 and 2011. At this time in the absence of any supporting data from a spectroscopic study or speckle interferometry it would be too early to assign any single reason or combination of phenomena that would unequivocally include the light travel time effect as an explanation to this very complex O-C diagram for AO Ser. A Roche model based on the W-D code provided a simultaneous theoretical fit of light curve data in three colors (B, V, and I_C). The photometric mass ratio estimated ($q = 0.235$) from W-D analyses is at odds with a theoretically computed value (0.45) published in 1980 (Brancewicz & Dworak), but consistent with that recently published by Yang et al (2010). Despite lacking critical spectroscopic or radial velocity data for this binary system, the light curve analysis herein based on a revised B-V color-index value for AO Ser provide strong evidence for an Algol-type binary system composed of an A7V main-sequence primary and K1 to K3 subgiant secondary.

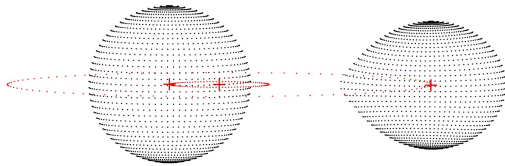


Figure 8. Three-dimensional rendering of the AO Ser binary system at phase 0.25.

This classification is much cooler than previously considered by all other investigators. Finally, Fourier analysis did not convincingly reveal any underlying periodicity other than that expected from the dominant orbital period. However, it is possible that the magnitude of any putative δ Sct-type pulsation is below the limits of detection for the equipment used in this investigation.

5. Acknowledgements

Special thanks are due to the NASA Astrophysics Data System hosted by the Computation Facility at the Harvard-Smithsonian Center for Astrophysics for providing convenient access to published literature. This research has also made use of the NASA/ IPAC Infrared Science Archive, which is operated by the Jet Propulsion Laboratory, California Institute of Technology, under

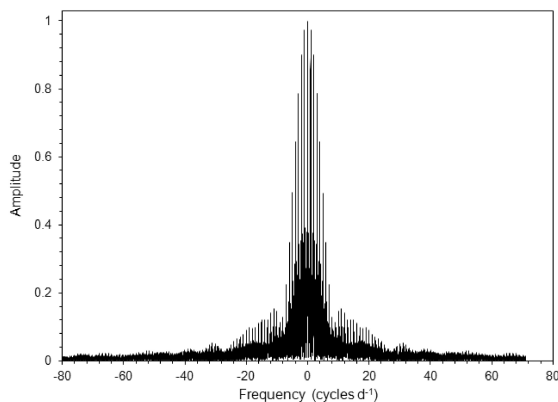


Figure 9. Spectral window for AO Ser exhibits strong sidebands offset by 1 cycle per day resulting from daily sampling aliases; results are shown for B-band residuals following Roche modeling, however, similar findings were observed in V and I_C.

contract with the National Aeronautics and Space Administration. The contribution of all the dedicated folks contributing to or managing the variable star time-of-minima data housed at the AAVSO, B.R.N.O., BBSAG, VSOLJ, and IBVS websites is gratefully acknowledged. This investigation has also made use of the SIMBAD database, operated at CDS, Strasbourg, France and the Bundesdeutsche Arbeitsgemeinschaft für Veränderliche Sterne (BAV) website in Berlin, Germany.

6. References

- Alton, K.B. 2010, "A Unified Roche-Model Light Curve Solution for the W UMa Binary AC Bootis", JAAVSO 38.
- Applegate, J.H. 1992, "A mechanism for orbital period modulation in close binaries." ApJ, 385, 621.
- Baldwin, M. & Samolyk, G. 2007, "Observed Minima Timings of Eclipsing Binaries No. 12." AAVSO, Cambridge, MA.
- Biermann, P. & Hall, D.S. 1973, A&A, 27, 249.
- Borkovits, T., Van Cauteren, P., Lampens, P., et al. 2008, "New and Archive Times of Minima of Eclipsing Binary Systems." IBVS, 5835, 3.
- Bradstreet, D. H. & Steelman D. P. 2002, "Binary Maker 3.0 - An Interactive Graphics-Based Light Curve Synthesis Program Written in Java." Bull. A.A.S., 34, 1224.
- Brancewicz, H. K. & Dworak, T. Z. 1980, "A catalogue of parameters for eclipsing binaries." Acta Astron., 30, 4, 501.
- Brát, L., Zejda, M. & Svoboda, P. 2007, "B.R.N.O. Contributions #34." Open Eur. J. Var. Stars, 74, 65.
- Brát, L., Šmelcer, L., Kučáková, H., et al. 2008, "B.R.N.O. Times of minima." Open Eur. J. Var. Stars, 94.
- Breger, M. 2000, "Asteroseismology of Delta Scuti Stars." Balt. Astron. 9, 149.
- Breger, M., Stich, J., Garrido, R., et al 1993, "Nonradial Pulsation of the Delta-Scuti Star BU Cancri in the Praesepe Cluster." A&A, 271, 482
- Budding, E. & Demircan O. 2007, "Introduction to Astronomical Photometry", Cambridge University Press, New York.
- Christiansen, J. L., Derekas, A., Ashley, M. C. B., et al. 2007, "The first high-amplitude δ Scuti star in an eclipsing binary system." MNRAS, 382, 1, 239.
- Diethelm, R. 2009, "Timings of Minima of Eclipsing Binaries." IBVS, 5894, 7.
- Diethelm, R. 2011, "Timings of Minima of Eclipsing Binaries." IBVS, 5992, 16.
- Doğru, S. S., Erdem, A., Dönmez, A., et al. 2009, "New Times of Minima of Some Eclipsing Binary Stars." IBVS, 5893, 2.
- Doğru, S. S., Erdem, A., Aliçavuş, F., et al. 2011, "CCD Times of Minima of Some Eclipsing Variables." IBVS, 5988, 2.
- Eddington, A.S. 1926, "The reflection effect in eclipsing variables." MNRAS, 86, 320.
- Fitzgerald, M.P. 1970, "The Intrinsic Colours of Stars and Two-Colour Reddening Lines." A&A, 4, 234.
- Flower, P.J. 1996, "Transformations from Theoretical Hertzsprung-Russell Diagrams to Color-Magnitude Diagrams: Effective Temperatures, B-V Colors, and

- Bolometric Corrections." *ApJ*, 469, 355.
- Ghedini, S. 1981, "A method for evaluating the epoch of minimum of an eclipsing variable - the sliding integrations." *Societa Astronomica Italiana*, 52, 633.
- Hall, D.S. 1989, "The relation between RS CVn and Algol." *Space Science Reviews*, 50, 219.
- Hamme, W. van 1993, "New limb-darkening coefficients for modeling binary star light curves." *ApJ*, 106, 2096.
- Harmanec, P. 1988, "Stellar masses and radii based on modern binary data." *Bull. Astron. Inst. Czechosl.*, 39, 329.
- Hoffmeister, C. 1935, "162 neue Veräderliche." *Astron. Nachr.*, 255, 401.
- Hübscher, J., Lehmann, P. B., Monninger, G., et al 2010, "BAV-Results of Observations - Photoelectric Minima of Selected Eclipsing Binaries and Maxima of Pulsating Stars." *IBVS*, 5918, 10.
- İbanoğlu, C., Soyduğan, F., Soyduğan, E. & Dervişoğlu, A. 2006, "Angular momentum evolution of Algol binaries." *MNRAS*, 373, 435.
- Koch, R. H. 1961, "Times of minimum light for several eclipsing binaries." *AJ*, 66, 35.
- Kim, S.-L., Kang, Y. B., Koo, J.-R., et al 2004, "Discovery of a short-periodic pulsating component in the Algol-type eclipsing binary system AO Ser." *IBVS*, 5538, 1.
- Kreiner, J.M. 2004, "Up-to-Date Linear Elements of Eclipsing Binaries" *Acta Astron.*, 54, 207.
- Kwee, K.K. & Woerden, H. van 1956, "A method for computing accurately the epoch of minimum of an eclipsing variable." *B.A.N.*, 12, 327.
- Kwee, K.K. 1958, "Investigation of variations in the period of sixteen bright short-period eclipsing binary stars." *B.A.N.*, 14, 131.
- Lampens, P., Kleidis, S., Van Cauteren, P., et al. 2010, "New Times of Minima of 36 Eclipsing Binary Systems." *IBVS*, 5933, 3.
- Lenz, P. & Breger, M. 2005, "Periodo4 User Guide." *Commun. Asteroseismol.*, 146, 53.
- Lucy, L.B. 1967, "Gravity-Darkening for Stars with Convective Envelopes." *Z. Astrophys.*, 65, 89.
- Manzoori, D. 2008, "The O-C curve analysis and simultaneous light curve solutions of classical Algol system U Cephei." *Ap&SS*, 318, 57.
- Mikuž, H., Dintinjana, B., Prša, A., et al. 2002, "Period Change and Surface Activity of the Eclipsing Binary UV Leonis." *IBVS*, 5338.
- Mkrtychian, D. E., Kusakin, A. V., Rodriguez, E., et al. 2004, "Frequency spectrum of the rapidly-oscillating mass-accreting component of the Algol-type system AS Eri." *A&A*, 419, 1015.
- MPO Canopus ©1996-2008, MPO Canopus & PhotoRed Installation Guide and Reference Manual, Bdw Publishing, Colorado Springs, CO 80908.
- Nelson, R.H. 2007, "Minima©2002, 2006: "Astronomy Software by Bob Nelson" URL: <http://members.shaw.ca/bob.nelson/software1.htm>.
- Parimucha, Š., Dubovský, P., Baludanský, D., et al 2009, "Minima Times of Selected Eclipsing Binaries." *IBVS*, 5898, 8.
- Pop, A. 2005, "On the Orbital Period Modulation of the Eclipsing Binary System Y Leonis." *Proceedings of ASP Conference Series*, 335, 263.
- Press, W., Teukolsky, S.A., Flannery, B.P. & Vetterling, W.T. 1992, "Numerical Recipes in FORTRAN" Cambridge: Cambridge Univ. Press.
- Prša, A. & Zwitter, T. 2005, "A Computational Guide to Physics of Eclipsing Binaries. I. Demonstrations and Perspectives." *ApJ*, 628, 1, 426.
- Qian, S. 2002, "Orbital Period Studies of Two Algol-Type Eclipsing Binary Systems: TY Pegasi and X Trianguli." *PASP*, 114, 650.
- Rensbergen, W. De Greve van, J.P. Mennekens, N., et al, 2011, "Mass loss out of close binaries. II." *A&A*, 528, A16.
- Rucinski, S.M. 1969, "The Proximity Effects in Close Binary Systems. II. The Bolometric Reflection Effect for Stars with Deep Convective Envelopes." *Acta Astron.*, 19, 245.
- Samolyk, G. 2008, "Recent Minima of 184 Eclipsing Binary Stars." *JAAVSO*, 36, 186.
- Samolyk, G. 2010, "Recent Minima of 161 Eclipsing Binary Stars." *JAAVSO*, 38, 85.
- Samolyk, G. 2011, "Recent Minima of 144 Eclipsing Binary Stars." *JAAVSO*, 39, 94.
- Schlegel, D., Finkbeiner, D. & Davis, M. 1998, "Application of SFD Dust Maps to Galaxy Counts and CMB Experiments." *Wide Field Surveys in Cosmology*, 14th IAP Mtg held May 26-30, Paris.
- Schwarzenberg-Czerny, A. 1996, "Fast and Statistically Optimal Period Search in Uneven Sampled Observations." *Ap J*, 460, L107.
- Surkova, L.P. & Svechnikov, M.A. 2004, "Semi-detached eclipsing binaries (Surkova+, 2004)." *VizieR On-line Data Catalog*: V/115.
- Warner, B. 2007, "Initial Results of a Dedicated H-G Project." *Minor Planet Bulletin*, 34, 113.
- Wilson, R.E. & Devinney, E.J. 1971, "Realization of Accurate Close-Binary Light Curves: Application to MR Cygni." *ApJ*, 166, 605.
- Wilson, R.E. 1979, "Eccentric orbit generalization and simultaneous solution of binary star light and velocity curves." *ApJ*, 234, 1054.
- Yang, Y.-G., Hu, S.-M., Guo, D.-F., Wei, J.-Y. & Dai, H.-F. 2010, "Photometric Properties for Selected Algol-type Binaries. II. AO Serpentis and V338 Herculis." *AJ*, 139, 1360.
- Zavros, P., Tstantilas, S. & Rovithis-Livaniou, E. 2008, "AO Serpentis: Observations and Interpretations." *Romanian Astronomical Journal*, 18, Suppl. 113.
- Zeipel, H. von 1924, "Radiative equilibrium of a double-star system with nearly spherical components." *MNRAS*, 84, 702.